Supplementary Information

Electrification of gasification-based Biomass-to-X processes - A Critical Review and in-depth Assessment

Marcel Dossow*[,a], Daniel Klüh*[,b], Kentaro Umeki[a,c], Matthias Gaderer[b], Hartmut Spliethoff[a], Sebastian Fendt[a]

[a] Technical University of Munich, Chair of Energy Systems, Boltzmannstr. 15, 85748, Garching b. München, Germany

[b] Technical University of Munich, Campus Straubing for Biotechnology and Sustainability, Professorship of Regenerative Energy Systems, Schulgasse 16, 93415 Straubing, Germany

[c] Luleå University of Technology, Department of Engineering Sciences and Mathematics, 97187 Luleå, Sweden

Content

1. Direct and indirect electrification technologies

In this section we present the processes which are not incorporated in the original paper. For the sake of completeness, the technologies are presented here in short. The technologies are of very low maturity, haven't gained much attention, or are less important in an electrified BtX process.

1.1. Indirect electrification (PBtX)

The following indirect electrification options are not presented in the paper, or in the case of H_2 addition not described in this level of detail provided here.

1.1.1. Hydrogen-heated metal alloy gasification

Another gasification concept (commercial technology HydroMax) is based on hot liquid metal alloys that convert biomass into syngas in a batch process [1]. The liquid alloys can be heated by the combustion of H_2 [1]. Dietenberger and Anderson present some more options of adding H_2 to the gasification process [1].

1.1.2. H_2 addition to synthesis

The available publications on indirectly electrified BtX processes by H_2 addition are chronologically elaborated in the following. Oulette and Scott first proposed H_2 addition before the catalytic synthesis step in 1995 [2]. The authors argue that syngas from biomass gasification contains excess carbon to produce MeOH. They proposed the addition of H_2 to biomass-based syngas for the production of MeOH [2]. In 1999, Specht et al. also investigated the MeOH production through allothermal steam gasification and the addition of H_2 before the synthesis unit [3]. Both early publications on PBtX processes use an estimation-based calculation approach arguing that there are only two ways to adjust the desired SN of the produced synthesis gas: CO_2 separation or H_2 addition. The latter enables almost complete utilization of the carbon contained in the biomass while simultaneously making use of the O_2 as a gasification agent in the gasification step. Thus, the carbon efficiency limitation of conventional BtX processes can be overcome, resulting in a high MeOH production rate [2,3].

Based on Specht et al., Mignard and Pritchard modeled an oxygen-blown stratified downdraft fixed bed gasification reactor using O_2 and H_2 from electrolysis in 2008 [4].They confirmed their predecessors' estimates of increased carbon efficiency and product yield with their calculation [4]. Also in 2008, Gassner and Maréchal investigated the integration of electrolysis in a wood-based BtX process to produce SNG [5]. They considered an indirectly heated, steam-blown fluidized bed gasifier and a directly heated, oxygen-blown fluidized bed gasifier as gasification technologies using a thermodynamic energy-flow model, coupled with an energy-integration model [5].

Multiple options for electrification of BtX processes were proposed by Agrawal and Sing in 2009 [6]. They reasoned that since a stand-alone BtX process generally could not recover more than 50% of the carbon from the biomass, additional energy in the form of heat, H_2, or electricity is required [6]. Using additional solar energy in the form of heat, H_2, or electricity two to three times more liquid fuel could be produced from a given amount of biomass compared to a stand-alone BtX process [6]. They also proposed an integrated process of H_2 addition and biological fermentation, in which the heat of the gasification-based process is used to provide process heat for the fermentation process and the CO_2 generated during fermentation is converted into liquid fuel [7]. Hertwich and Zhang also modelled the integration of solar energy in the form of heat and H_2 from electrolysis into a biomass steam gasification process to produce MeOH [8]. In 2010, Agrawal and Singh presented an overview of the several BtX fuel conversion processes that treat biomass primarily as a carbon source and significantly increase liquid fuel production by utilizing additional energy as heat, electricity, or H_2 [9]. Using the principles of this proposed process, Baliban et al. modeled a PBtX process employing a CFB gasifier with subsequent H_2 addition to a rWGS unit to obtain almost 100% carbon efficiency towards FT fuels [10].

In 2010, Seiler et al. investigated 'Enhanced Biomass-to-Liquid' (EBtL): BtX processes with external energy inputs to increase fuel production significantly [11]. They compare slow pyrolysis, fast pyrolysis, and torrefaction with subsequent milling as pretreatment for the EFG. For the EFG four alternatives for energy input are considered, including an oxygen-/air-blown autothermal reactor, and three allothermal reactor options (plasma heating, co-combustion of H_2, co-combustion of natural gas). For syngas cooling, a simple quench

option is compared to a chemical quench and a heat recovery. In terms of gas conditioning, Tectisol and water-amine cleaning are considered in combination with a WGS or H_2 from either water electrolysis or natural gas reforming.

Clausen et al. conducted a detailed process simulation in 2010 comparing six MeOH production routes, each with a different syngas production method, including one with a two-stage fluidized bed gasifier for biomass conversion and H_2 addition [12]. In 2011, the same group published a more advanced modeling approach on MeOH plants based on combining water electrolysis and EFG of torrefied biomass [13]. Here, part of the H_2 is used as a chemical quench for the EFG, with the rest being mixed with the cleaned syngas before synthesis, while the produced O_2 is used as gasification agent in the EFG.

Mallapragada et al. present a detailed systems analysis of the transportation sector with an energy efficiency roadmap as requested in 2010 [14,15]. The analysis is based on using renewable carbon sources like biomass and atmospheric CO_2, solar energy in the form of H_2, heat, and electricity, in conjunction with novel processes for producing liquid fuels [15]. In 2012, Bernical et al. published their first preliminary investigation of an H_2 enhanced BtX process to produce FT fuels. Comparing high-temperature steam electrolysis (SOEL) and AEL in a highly integrated process, they conclude that the use of SOEL almost doubles the product yield while achieving significant electricity savings [16,17].

Ridjan et al. also investigated an H_2-enhanced BtX process with steam electrolysis using oxygen-blown gasification to produce MeOH or steam gasification to produce SNG based on the CEESA project [18]. They also investigated a co-electrolysis option, which does not rely on syngas as feed and is therefore not included in this review. In 2014, Clausen et al. investigated (P)BtX processes using torrefaction as pretreatment to an EFG. Torrefaction is either done in decentralized plants or in a central plant [19]. They found that the integration of torrefaction benefits most from the integration of electrolysis compared to other process configurations[20].

Hannula compared the BtX route, to a pure PtX process and to a combined PBtX route [21]. Using an AEL and a CFB they modelled the PBtX process pathways producing SNG or MeOH with the optional MeOH-to-gasoline conversion [21]. In 2016, Hannula's research focused more on the PBtX approach maximizing the potential to increase fuel production [22]. Process options include using oxygen-blown or steam-blown gasification coupled with an AEL for SNG or gasoline production via the MeOH-to-Gasoline route [22]. In 2016, Trop and Goricanec also simulatively compared the production of MeOH and SNG from torrefied biomass via EFG and the addition of H_2 from electrolysis before the synthesis step [23]. König et al. also conducted a techno-economic case study on green FT fuels, including a PBtX process using a slurry-fed entrained flow gasifier and PEMEL [24–26]. Furthermore, Nikparsa et al. proposed a process using the Güssing dual fluidized bed steam gasifier, adding H_2 to reach the required SN of 2 before FT synthesis [27].

In 2017, Koponen and Hannula investigated the GHG emissions of the H_2 enhanced BtX process designs [28]. As mentioned above, Onarheim et al. investigated a pyrolysis-based process where the carbon conversion was maximized by producing SNG from the bio-oil production process off-gases adding H_2 [29]. Catalytic methanation of process off-gases using additional H_2 from water electrolysis boost the overall process efficiency. Clausen modeled a PBtX using a generic biomass feedstock with varying ash and water content to produce SNG [30]. The process is composed of an SOEL unit coupled with a two-stage gasifier. This so-called "Viking" gasifier consists of a first stage where the biomass feedstock is pyrolyzed and partially oxidized by adding air or O_2 to lower the tar content. In the second stage, the gas passes through a downdraft fixed bed gasifier primarily gasifying the char from the pyrolysis stage [31–33]. In 2018, Sigurjonsson and Clausen investigated a process design that enables SNG and heat production from biomass by integrating electricity in the form of H_2 when operating in electricity storage mode in times of low electricity prices [34]. With a rSOC cell, the system can also generate electricity from biomass-derived syngas when electricity prices are high [34].

Also, Firmansyah et al. conducted a simple mass and energy balance calculations for a MeOH producing PBtX process [35]. The process design comprises of a fixed bed gasifier combined with a AEL unit and H_2 addition before MeOH synthesis. In 2019, Anghilante et al. also modeled several PBt-SNG concepts using fixed bed gasification of various biomasses coupled with either PEMEL or SOEL [36]. In their work, SNG is directly upgraded to either compressed SNG (CNG), or liquefied SNG (LNG).

Using an EFG coupled with a SOEL, Hillestad et al. modeled a PBtX process in 2018 [37]. With their three-stage FT reactor set up and H_2 addition to each stage, the rWGS reactor and the upgrading section, they enable a high carbon efficiency of more than 90%. In 2019, Ostadi et al. conducted an exergy analysis on this PBtX process, determining the exegetic efficiency to be 69% [38]. In the same year, the authors published another study investigating the impact of the H_2/CO ratio to the FT reactors on the production and power consumption concluding that optimum conditions in terms of power required per extra produced liter fuel are at a H_2/CO feed ratio significantly lower than 2 [39]. Subsequently, Ostadi et al. conducted a parametric optimization of their staged process in terms of H_2/CO ratios, reactor volumes, and gasification conditions [40]. In a recently published study, Nielsen et al. investigated the same PBtX process redirecting the tail gas of the FT reactor to the anode of an SOEL to serve as fuel [41]. Supplying fuel to an SOEL aims to lower the electrical work input required for SOEL to increase energy efficiency of fuel production to more than 90%. Kurkela et al. also investigated a PBtX process to flexibly produce heat, power and FT fuel from biomass gasification while seasonally using H_2 addition from solar power [42]. The experimental development will be carried out using a 1 MW_{th}, pressurized, fixed-bed gasification pilot plant.

Zhang et al. also investigated a PBtX process producing MeOH employing an EFG coupled with a SOEL [43]. In 2020, Zhang et al. conducted a techno-economic optimization for this process [44]. Subsequently, they compared a PBtX process with H_2 addition from SOEL with a process design using the SOEL in co-electrolysis mode both options featuring an EFG and producing either SNG, MeOH, DME or SAF via FT [45].

In 2021, Dossow et al. modeled a PBtX process using EFG coupled with H_2 and O_2 from water electrolysis, comparing PEMEL and SOEL to produce FT fuels [46]. The detailed process models show the high potential for increasing carbon efficiency to up to 97% by integrating renewable power into the BtX process [46].

In 2020, Butera et al. introduced a gasification concept with a straw-based low-temperature CFB gasifier, a POX unit and hot wood char bed unit to reduce the tar concentration, coupled with a SOEL unit [47]. Based on this work, Kofler and Clausen investigated two process options to produce SNG or DME combining the low-temperature CFB with an AEL unit for H_2 addition before synthesis [48]. Their concept includes the so-called "PolyGas" approach, where part of the pyrolysis gas is not reformed and used for synthesis but is ejected as byproduct, making a comparison with other processes impossible.

Also in 2020, Butera et al. investigated the coupling of gasification with SOEL, comparing an FB gasifier, a BFB gasifier and an EFG for MeOH production [49]. The comparison comprises three system designs where the SOEL operates in co-electrolysis in-line processing the biomass-derived syngas. They use their two-stage electro-gasifier design, and two EFG options where H_2 is added to the syngas either as a chemical quench or upstream of the MeOH synthesis. Based on this work, Butera et al. techno-economically compared their two-stage electro-gasifier design with a PBtX process based on the more conventional two-stage gasifier design adding H_2 to the syngas before synthesis [50].

Furthermore, Poluzzi et al. investigated different PBtX process options using either an oxygen-blown and indirectly heated or an indirectly heated and sorption-enhanced fluidized bed gasifier with H_2 addition before the synthesis [51]. They published another study comparing different CFB reactor designs to evaluate the optimal design of a PBtX plant producing MeOH and operating both with and without H_2 addition [52].

In 2021, Giglio et al. investigated a PBtX process for SNG production [53]. Woody biomass is converted in a CFB gasification step and the product yield is enhanced using SOEL for H_2 production [53]. Also, Henning and Haase investigated a process producing gasoline via MeOH [54]. They used a slurry-fed EFG and AEL to produce MeOH and gasoline via the MeOH-to-gasoline process.

Also in 2021, Habermeyer et al. investigated a PBtX process using CFB and AEL similar to Hannula et al.'s work [22,55]. The concept allows to switch operation modes from PBtX with H_2 addition to BtX [55]. In 2022, Fournas and Wei also published their techno-economic results investigating a H_2-enhanced BtX process to produce MeOH [56]. Using torrefaction, EFG and PEMEL, they performed a techno-economic and GHG emission-based analysis. In 2022, Pandey et al. assessed four different PBtX process concepts for small-scale FT fuel production based on the integration of SOEL to BtX processes proposed by Hillestad et al. (2018) [57]. The proposed PBtX processes consider different SOEL integration options and points of H_2 addition: in two of the investigated PBtX cases rWGS is included and part of the H_2 is added to the rWGS reactor. Also, two of the cases include CO_2 removal via Selexol wash [57]. In 2023, Ostadi et al. conducted a techno-economic study, adding H_2 from either water electrolysis using SOEL or natural gas pyrolysis to enhance a MeOH producing PBtX process [58].

1.2. Direct electrification (eBtX)

In the following, we discuss technologies that are of very low maturity, haven't gained much attention, or are less important in an eBtX process. The section about co-electrolysis presents the cited studies from the paper in more detail.

1.2.1. Infrared, microwave-assisted and induction drying

Infrared drying is typically employed in surface drying and drying of thin sheets like textiles, paper, or paints [59,60]. It is also already commercialized for biomass drying [61]. To reach an efficient drying process, the radiation properties of the radiator and material for drying need to match [60]. However, infrared dryers are only surface dryers and unsuitable for the drying of thick beds [146]. Therefore, the applicability of infrared dryers for biomass drying is limited.

Microwave-assisted drying was experimentally tested for various biogenic feedstocks [62–64]. The literature on the energy consumption of microwave drying compared to conventional drying is contradictory [65–67]. The effect of microwave-assisted drying on biomass properties are, for example, changes in surface structure, surface area, pore volume, crystallinity, and more properties that would affect subsequent processes [68–70]. Additionally, combustion characteristics of food waste are improved by microwave compared to conventional drying [71]. No specific studies on the influence of microwave drying on gasification characteristics were found. Drying by induction was investigated by Xue et al. for sewage sludge using three different heat-dissipating materials [72]. This is the only publication on inductively-heated drying to the authors' knowledge.

1.2.2. Microwave-assisted torrefaction

Microwave-assisted torrefaction was tested for various feedstocks [67]. The energy yield is comparable to conventional processes [67]. Microwave-assisted torrefaction shows a processing time that is tremendously shorter than with conventional heating [67,73,74]. Ho et al. compared the conventional torrefaction with microwave-assisted torrefaction for coffee ground and microalga residues and concluded that microwave-assisted torrefaction is more energy efficient in comparison [74]. Mohd Fuad et al. state that microwave-assisted torrefaction is economically promising due to reduced processing time and energy input [73]. Additionally, fine grinding can be avoided when using microwave-assisted torrefaction [73]. First experiments on the gasification properties of products from microwave-assisted torrefaction are reported. The steam gasification performance of herb residues torrefied with microwave yielded a higher gas yield with a higher heating value and a lower tar content than the non-treated substrate and conventionally torrefied herb residues [75]. However, the additional energy released in gasification was leveled out by the energy required for microwave-assisted torrefaction.

1.2.3. Microwave-assisted HTC

In HTC, wet biomass is treated at elevated temperatures in a aqueous environment under elevated pressure [76]. Several studies have been conducted on microwave-assisted HTC of different biomass [77]. Like microwave-assisted torrefaction, the processing time can be reduced compared to conventional heating methods [78]. Elaigwu and Greenway concluded from their comparative experiments that the same conversion level can be reached after a processing time of 20 min for microwave-assisted HTC and 240 min for conventional HTC, both in batch mode [79]. Zhang et al. confirm a 5 to 10-fold processing time reduction for cellulose in microwave-assisted HTC [80]. According to Zulkornain et al., the heating value of hydrochar from microwave-assisted HTC is higher than in conventional processes [81]. Shao et al. compared microwave-assisted with HTC heated in an oven and oil bath [82]. They found an improvement in major properties (energy densification, carbon content, fuel ratio, combustion characteristics, adsorption, and energy requirement for the process) compared to conventional HTC. Nevertheless, there is still a lack of comparison of energy efficiency and economic evaluation between microwave-assisted and conventional HTC. So far, the influence of hydrochar produced by microwave-assisted HTC on the gasification process was not tested as it was already done for the gasification of hydrochar from conventional HTC (for example [83–85]).

For HTC and torrefaction, only lab experiments exist that use heating by induction due to simplicity and feasibility, not because of the technology [86–88].

1.2.4. Electron-assisted gasification

For process enhancement, electrons can be directly introduced to the gasifier. According to experimental studies, feeding electrons into the gasifier has positive effects on the process. Yang et al. experimentally investigated the impact of thermal electrons set free from a wire in fixed coal bed gasification [89,90]. Results show that thermal electrons increase carbon conversion at lower temperatures compared to a normal gasification process. Furthermore, the concentration of CO in the syngas increases with increasing electrical power input. Ismail et al. fed electrons to the biomass gasifier via the air feed [91]. They found positive effects like a faster thermal breakdown of the feedstock and accelerated H_2 and CO production. The efficiency and economics of electron-assisted gasification of biomass has not yet been quantified due to the low technical readiness and limited interest in this technology.

1.2.5. Microwave-assisted synthesis

In microwave-assisted synthesis, uniform and fast heating inside the reactor can be reached by applying MWs. The effect of MWs is only attributed to the direct heating and not any other influences of the MWs on the reaction. Most MW-assisted reactions occur in the liquid and solid phase [92–94]. However, heterogeneous catalyzed gas phase reactions like the oxidative coupling of methane, selective oxidation, reduction of SO_2 and NO_x [95], and methane reforming [96] are also investigated. Durka et al. give a good overview on MW-assisted gas phase reactions [97]. Since the syngas-based synthesis processes are exothermal, heat input to the reactor is not required; therefore, heating via MWs is not helpful.

Additionally, heating syngas with MWs is not effective. CO_2, CO, and H_2 exhibit weak or no dipole moments. Consequently, they are not absorbing the MW energy efficiently [98] compared to liquids like water, for example [94]. However, an absorption medium can efficiently transfer heat to the gas.

1.2.6. Direct reduction of CO

CO_2 and CO can be electrochemically reduced to molecules like ethylene, acetic acid, ethanol, or n-propanol. As discussed in literature, using CO as feedstock is beneficial compared to CO_2 [99]. Therefore, CO from syngas might be an interesting option compared to the direct reduction of CO_2 or the two-step reduction via CO_2 electrolysis as an intermediate process. Klüh et al. investigate the direct electrochemical reduction of CO to C_2 products from biomass syngas [100]. Comparing this path to the conventional two-step process connected to a biomass power plant with CO_2 capture, showed better energy efficiency and economics but lower carbon efficiency for the gasification-based routes. The ER is in the range of 1.8 to 1.9. Further studies in this field are not known.

1.2.7. Microbial electrosynthesis

In electro-biotechnological processes, syngas (CO as carbon and energy source being the most important component) can be either used to generate electricity or to produce valuable products by the addition of electrical energy (microbial electrosynthesis). Possible products include hydrogen, methane, acetate, ethanol,1,3-propanediol, 3-hydroxypropionic acid, lactate, butanol, 2,3-butanediol, butyrate, and acetone [242,243]. Microbial electrosynthesis comprises four major concepts of how electrical energy is delivered to the microbes with a TRL between low 2 and 7 [101]. To the authors' knowledge, an engineering-based economic or environmental evaluation with syngas as feedstock is unavailable in literature. However, first assessments for CO_2 as feedstock show that electricity and anode cost are the main drivers in these processes [102].

1.2.8. Inductively heated synthesis

The advantages of induction-heated synthesis processes are the high heating rates and, consequently short start-up times of the reactor when operated flexibly [103]. The process concept is investigated for FT and Methanation reaction [104].

2. Meta-Analysis

This section explains the mathematical derivation of the meta-analysis performed in Section 6 in the paper.

2.1. General KPI definitions

The following equations show the KPIs as already defined in Section 1 of the paper.

$$\eta_C = \frac{\dot{m}_{C,product}}{\dot{m}_{C,biomass}} \tag{1}$$

$$PY = \frac{\dot{m}_{product}}{\dot{m}_{biomass,dry}} = \frac{\dfrac{\dot{m}_{C,product}}{w_{C,product}}}{\dfrac{\dot{m}_{C,biomass,dry}}{w_{C,biomass,dry}}} = \eta_C \cdot \frac{w_{C,biomass,dry}}{w_{C,product}} \tag{2}$$

$$EY = \frac{E_{prod}}{E_{feed}} = \left\{ \begin{array}{ll}
\dfrac{\dot{m}_{product} \cdot LHV_{product}}{\dot{m}_{biomass} \cdot LHV_{biomass}} & (BtX) \\[3mm]
\dfrac{\dot{m}_{product} \cdot LHV_{product}}{P_{electrolysis}} & (PtX) \\[3mm]
\dfrac{\dot{m}_{product} \cdot LHV_{product}}{\dot{m}_{biomass} \cdot LHV_{biomass} + P_{electrolysis}} & (PBtX) \\[3mm]
\dfrac{\dot{m}_{product} \cdot LHV_{product}}{\dot{m}_{biomass} \cdot LHV_{biomass} + P_{el.direct}} & (eBtX)
\end{array} \right. \tag{3}$$

$$ER = \frac{P_{el}}{E_{biomass}} = \left\{ \begin{array}{ll}
\dfrac{P_{electrolysis}}{\dot{m}_{biomass} \cdot LHV_{biomass}} & (PBtX) \\[3mm]
\dfrac{P_{el.direct}}{\dot{m}_{biomass} \cdot LHV_{biomass}} & (eBtX)
\end{array} \right. \tag{4}$$

2.2. Mathematical derivations

Equation (5) shows the linear relation of the BtX energy yield. The slope is represented by the energy yield of the PtX process either with high or low temperature electrolysis ($\overline{EY}_{PtX,LT/HT}$). The intersection with the y-axis is the energy yield of the BtX process ($\overline{EY}_{BtX}$).

$$EY_{BtX \to PBtX} = \frac{\dot{m}_{product} LHV_{product}}{\dot{m}_{biomass} LHV_{biomass}} = f(ER) = \overline{EY}_{BtX} + \overline{EY}_{PtX,LT/HT} * ER \tag{5}$$

With the definition of the EY_{BtX}, Equation (6) represents the mathematical equation for the product yield. EY_{BtX} is the substituted by Equation (5).

$$PY_{BtX \to PBtX} = \frac{\dot{m}_{product}}{\dot{m}_{biomass,dry}} = f(ER) = \frac{LHV_{biomass}}{LHV_{product}} \cdot (\overline{EY}_{BtX} + \overline{EY}_{PtX,LT/HT} * ER) \tag{6}$$

The carbon efficiency can also be mathematically derived based on Equation (2) and (6).

$$\begin{aligned}
\eta_{C,BtX \to PBtX} &= \frac{\dot{m}_{C,product}}{\dot{m}_{C,biomass}} = PY \cdot \frac{w_{C,product}}{w_{C,biomass,dry}} = f(ER) \\
&= \frac{LHV_{biomass}}{LHV_{product}} \frac{w_{C,product}}{w_{C,biomass,dry}} \cdot (\overline{EY}_{BtX} + \overline{EY}_{PtX,LT/HT} * ER)
\end{aligned} \tag{7}$$

$$EY_{PtX \to PBtX} = \frac{\dot{m}_{product}LHV_{product}}{E_{electr.}} = f(ER) = \frac{EY_{BtX \to PBtX}}{ER} = \overline{EY}_{PtX,LT/HT} + \frac{\overline{EY}_{BtX}}{ER} \tag{8}$$

$$\begin{aligned} EY_{PBtX} &= \frac{\dot{m}_{product}LHV_{product}}{\dot{m}_{biomass}LHV_{biomass} + E_{electr.}} = f(ER) \\ &= \frac{\dot{m}_{product}LHV_{product}}{\dot{m}_{biomass}LHV_{biomass}(1 + ER)} = \frac{EY_{BtX \to PBtX}}{1 + ER} = \frac{\overline{EY}_{BtX} + \overline{EY}_{PtX,LT/HT} \cdot ER}{1 + ER} \end{aligned} \tag{9}$$

Table 1: KPIs of BtX and PtX processes as reference for meta-analytical evaluation of PBtX processes

KPI	Unit	SNG	MeOH	FT	Ref.
$\overline{EY}_{BtX}$	$MW_{product} MW_{biomass}^{-1}$	0.57	0.59	0.40	[105]
$\overline{EY}_{PtX,LT}$	$MW_{product} MW_{electrolysis}^{-1}$	0.52	0.55	0.45	[106]
$\overline{EY}_{PtX,HT}$	$MW_{product} MW_{electrolysis}^{-1}$	0.84	0.75	0.59	[107,108]
$\overline{EY}_{PtX,co-electrolysis}$	$MW_{product} MW_{electrolysis}^{-1}$	0.83	0.79	0.65	[107,108]
$\overline{\eta}_{C,BtX}$	%	32%	40%	36%	[105]
$\eta_{C,BtX \to PBtX}(ER = 0)_{\mathbf{a}}$	%	31%	34%	30%	
$\overline{PY}_{BtX}$	$kg_{product} kg_{biomass,dry}^{-1}$	0.25	0.59	0.23	[105]
$\overline{PY}_{BtX \to PBtX}(ER = 0)$	$kg_{product} kg_{biomass,dry}^{-1}$	0.21	0.53	0.17	

2.2.1. Supplementary Graphs

Figure 1: Dependency of electrification ratio ER on a)-c) carbon efficiency and d)-e) product yield for PBtX processes using H_2 addition to synthesis (and rWGS) to produce synthetic natural gas (SNG), Methanol (MeOH) or Fischer-Tropsch (FT) products based on literature review including the derived equations for $PY_{BtX \rightarrow PBtX}$ (Equation (6)) and $\eta_{C,BtX \rightarrow PBtX}$ (Equation (7)) based on high-temperature (HT) or low-temperature (LT) PtX reference processes. PBtX studies using H_2 addition from water electrolysis include the use of alkaline (AEL), proton exchange membrane (PEMEL), or solid oxide electrolysis (SOEL). For data basis see Section 2.3.
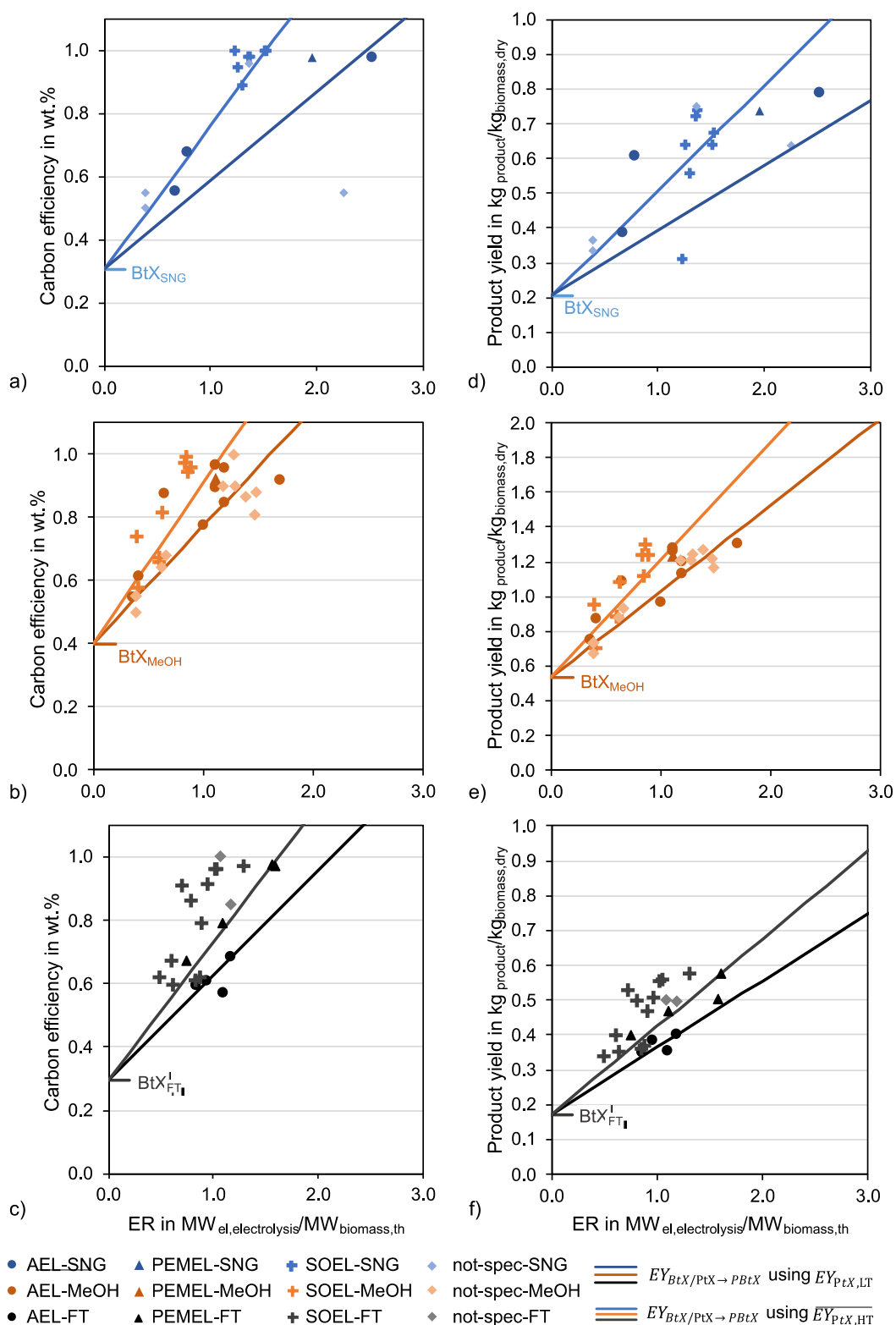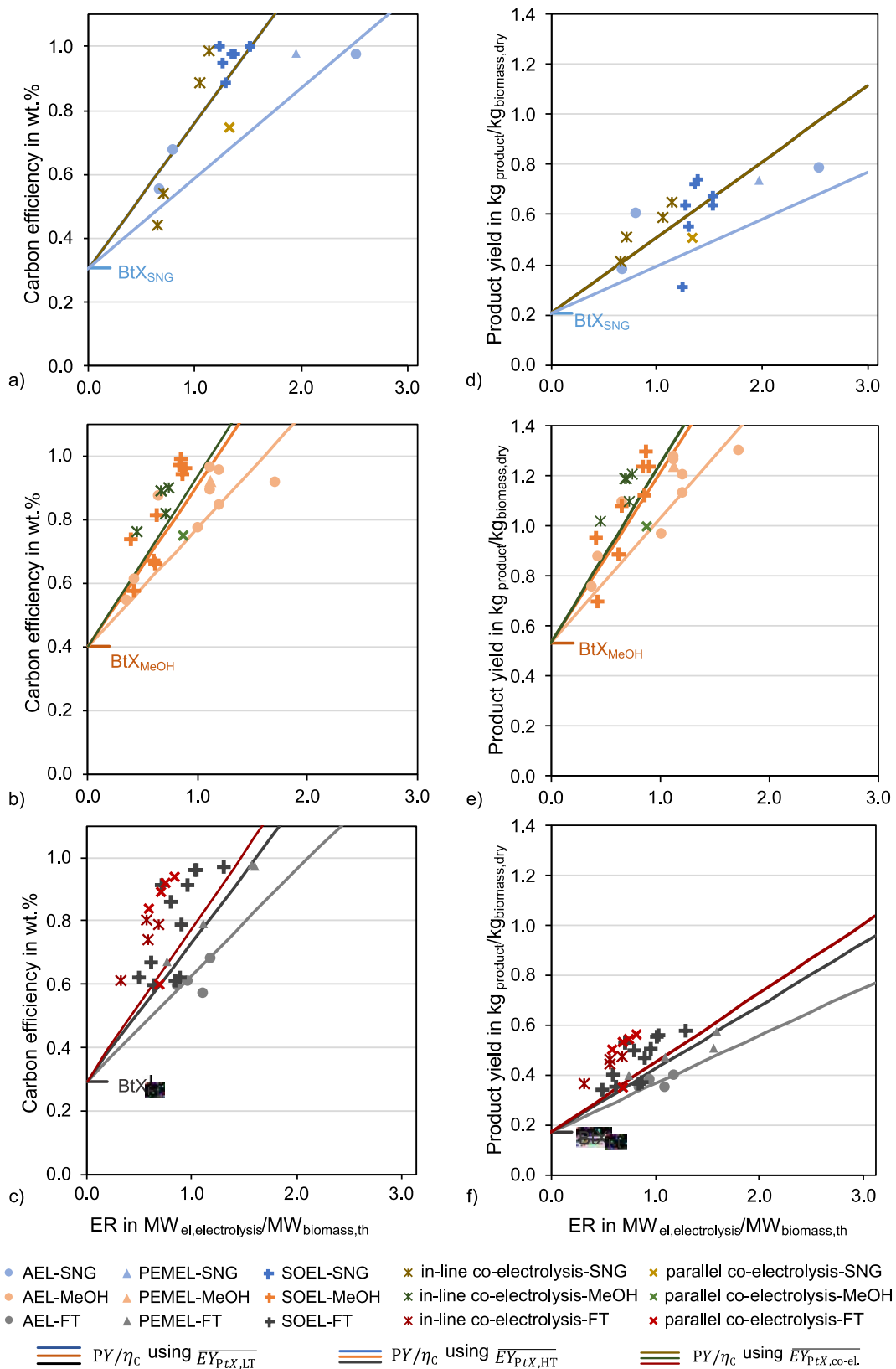
Figure 2: Dependency of electrification ratio ER on a)-c) carbon efficiency and d)-f) product yield for PBtX processes using H_2 addition to synthesis (and rWGS), and parallel (PBtX) and in-line (eBtX) integration of co-electrolysis to produce synthetic natural gas (SNG), Methanol (MeOH) or Fischer-Tropsch (FT) products based on literature review based on literature review including the derived equations for $PY_{BtX \rightarrow PBtX}$ (Equation (6)) and $\eta_{C,BtX \rightarrow PBtX}$ (Equation (7)) based on high-temperature (HT) or low-temperature (LT) or co-electrolysis (co-el.) PtX reference processes. PBtX studies using H_2 addition from water electrolysis included use alkaline (AEL), proton exchange membrane (PEMEL), or solid oxide electrolysis (SOEL). Studies that do not specify the used electrolysis technology are neglected. For data basis see Section 2.3.
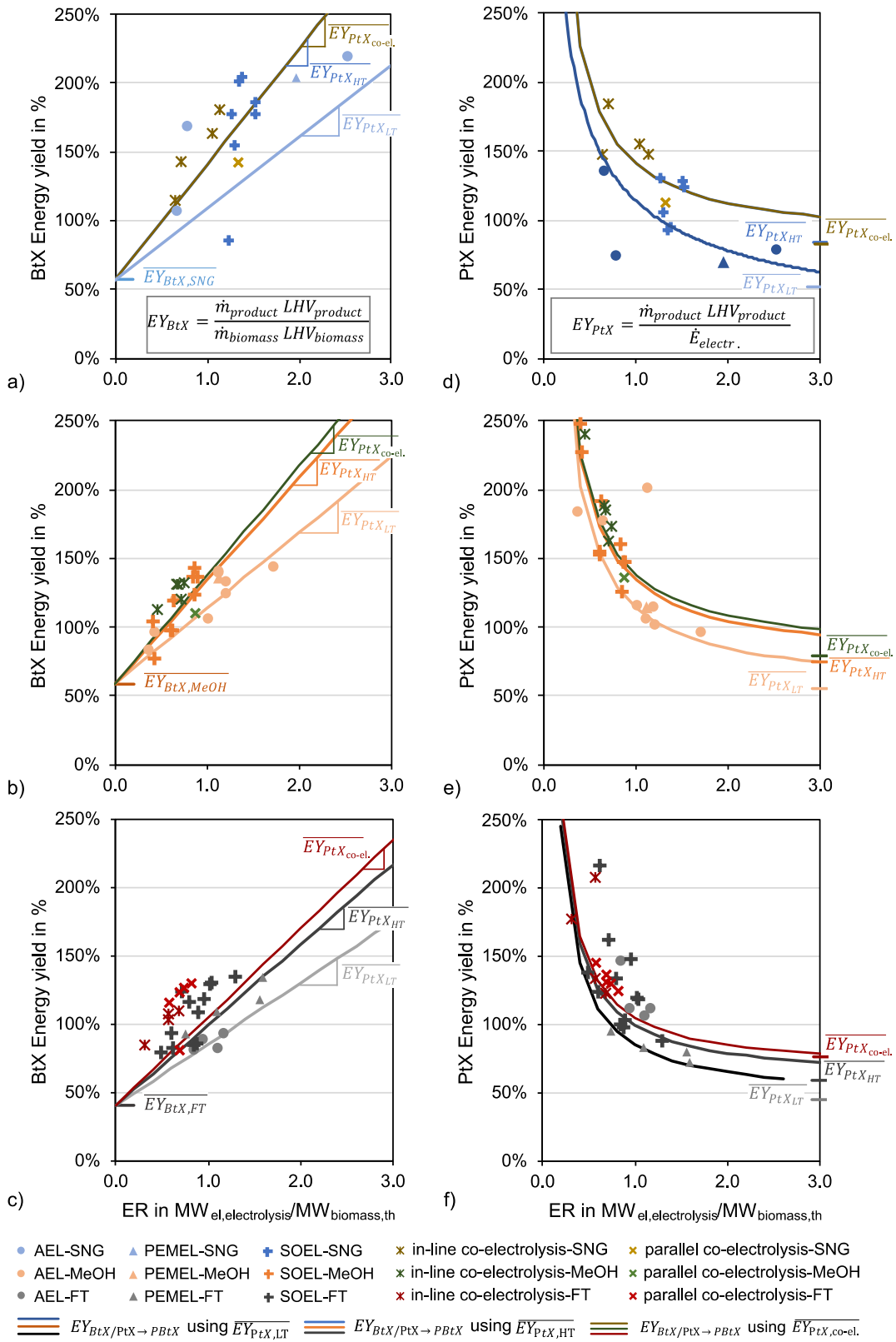
Figure 3: Dependency of electrification ratio ER on a)-c) BtX energy yield and d)-e) PtX energy PY for PBtX processes using H₂ addition to synthesis (and rWGS)), and parallel (PBtX) and in-line (eBtX) integration of co-electrolysis to produce synthetic natural gas (SNG), Methanol (MeOH) or Fischer-Tropsch (FT) products based on literature review including the derived equations for $PY_{BtX \to PBtX}$ (Equation (6)) and $\eta_{C,BtX \to PBtX}$ (Equation (7)) based on high-temperature (HT), low-temperature (LT), or co-electrolysis (co-el.) PtX reference processes. PBtX studies using H₂ addition from water electrolysis include the use of alkaline (AEL), proton exchange membrane (PEMEL), or solid oxide electrolysis (SOEL). Studies that do not specify the used electrolysis technology are neglected.

2.3. Data Overview from Literature Research

The following tables show the data of available process simulations for hydrogasification (Table 2), electrically-heated gasification (Table Table),H_2 addition to the synthesis for SNG (Table), MeOH (Table 5) and FT (Table 6). Some tables are similarly included in the paper. However, the tables here contain additional information also for already included tables in the paper.

Table 2 provides an overview of available PBtX process simulation studies using hydrogasification via H_2 addition to produce SNG. KPIs such as EY, η_C, and PY are not included in the meta-analytic assessment in the main paper, due to the limited data availability. ER is shown in Figure 15 in the main paper.

Table 2: Summary of literature on Power-and-Biomass-to-SNG process simulation studies using hydrogasification including the used gasification and electrolysis technologies used in Figure 15 in main paper. KPI values derived from the data in the papers.

Reference	Plant Size Biomass input / Electrical power to electrolysis	Biomass Feedstock	Pretreatment	Gasifier	Syngas cleaning	Reformer	Electrolyzer	ER MW$_{el}$/MW$_{th}$	PY kg$_{SNG}$/kg$_{BM,dry}$	η_C %	EY %
Mozaffarian et al. 2002 [109]	20 MW$_{th,LHV}$ / 27.4 MW$_{el}$	willow wood	Dryer	fluidized bed	low temp. gas cleaning	Not specified	Not specified	1.45	0.73	80%	63%
Barbuzza et al. 2019 [110]	1.41/1.41/1.41 MW$_{th,LHV}$ / 1.39/0.19/1.52 MW$_{el}$	woody biomass	not specified	not specified	Not specified	PSA[a]	SOEL[a]	0.99/0.13/1.08	0.70/0.34/0.67	95%/45%/99%	83%/62%/66%

[a]: PSA: Pressure swing adsorption, SOEL: Solid oxide electrolysis

Table 3: Summary of literature on eBtX process simulation studies used in Figure 15 in main paper that employ electrically-heated gasification including the used gasification technologies. KPI values derived from the data in the papers.

Reference	Plant Size Biomass input / Electrical power to heater	Biomass Feedstock	Pretreatment	Gasifier	ER MW$_{el}$/MW$_{th}$	Product
Butera et al. 2020 [49]	100/100 MW$_{th,LHV}$ / 11.3/15.8 MW$_{el}$	woody biomass	steam dryer + milling	EFG[a]	0.113/0.158	MeOH
Song et al. 2022 [111]	109 MW$_{th,LHV}$ / 31 MW$_{el}$	Wheat straw	dryer	not spec	0.284	SNG

[a]: EFG: Entrained flow gasification

The assessment of KPIs for the study by Putta et al. who carried out process simulations for the PBtX system with an electrically-heated EFG and H_2 addition from SOEL [112] was not possible because it shows only economic indicators of the plant.

Table 4: Literature overview for Power-and-Biomass-to-SNG studies including the scope, plant size, the used pretreatment, gasification, syngas cleaning, reforming, and electrolysis technologies. KPI values derived from the data in the respective literature.

Reference	Scope[a]	Plant Size Biomass input / Electrical power to electrolysis	Biomass Feedstock	Pretreatment	Gasifier[b]	Syngas cleaning	Reformer	Electrolyzer[c]	ER MW_{el}/MW_{th}	PY $kg_{SNG}/kg_{biomass,dry}$	η_C %	EY_{PBtX} %	EY_{BtX} %	EY_{PtX} %
Gassner and Maréchal 2008 [5]	P	20 MW$_{th,LHV}$ / 27.4 MW$_{el}$	Wood chips	steam drying	CFB	Cold gas clean-up (filter, scrubber, guard beds)	steam reforming	not specified	1.37	0.75	100%	75%	208%	116%
Ridjan et al. 2013 [18]	E	Not specified	Not specified	Not specified	Not specified	Not specified	Not specified	SOEL	1.26	0.64	95%	75%	178%	131%
Hannula 2015 [21]	P	100 MW$_{th,LHV}$ / 65.8 MW$_{el}$	Forest residues chips	Belt drier	CFB	filter, sour WGS, water scrubber, AGR (MeOH/rectisol wash), guard beds	catalytic reformer	AEL	0.66	0.39	56%	60%	108%	137%
Hannula 2016 [22]	P	100 MW$_{th,LHV}$ / 252 MW$_{el}$	Forest residues chips	Belt drier	CFB	filter , water scrubber, AGR (MeOH/Rectisol wash), guard beds	catalytic reformer	AEL	2.52	0.79	98%	58%	221%	79%
Trop and Goricanec 2016 [23]	P	600 MW$_{th,LHV}$ / 1355.2 MW$_{el}$	Torrefied biomass wood chips, switch grass, manure, sewage sludge etc.)	Mill Dryer	EFG	AGR (Selexol)	-	not specified	2.26	0.64	96%	54%	177%	78%
Clausen 2017 [30]	P	5.0 MW$_{th,LHV}$ / 6.2 MW$_{el}$	(Torrefied... switch grass, manure, sewage sludge etc.)	steam drying + pyrolysis	TSG	-	-	SOEL	1.24	0.31	100%	74%	86%	532%
Sigurjonsson and Clausen 2018 [34]	P	89 MW$_{th,LHV}$ (100 MW$_{th,LHV}$ to gasifier) / 135.6 MW$_{el}$	Wood chips	steam drying + pyrolysis	TSG	bag house filter + sulfur guard	-	SOEL	1.52	0.64	100%	75%	178%	129%
Anghilante et al. 2019 [36]	P	9.7/9.5/9.5 MW$_{th,LHV}$ / 13/19/13 MW$_{el}$	Wood, straw, sewage sludge	air drying	FB	Hot gas & fine cleaning	-	SOEL/SOEL/ PEMEL	1.35/1.38/ 1.96	0.72/0.74/ 0.74	98%/98%/ 98%	64%/65%/ 52%	205%/205%/ 201%	70%/95%/ 94%
Zhang et al. 2020 [45]	P	10 MW$_{th,LHV}$ / 13 MW$_{el}$	woody biomass	-	EFG	AGR (MEA)	-	SOEL	1.3	0.557	89%	63%	155%	106%
Poluzzi et al. 2020 [51]	P	Not specified	woody biomass	Drying	CFB/DFB/ SEG[d]	WGS + cleaning + AGR	-	not specified	0.39 (3)	0.37/0.37/ 0.33	55%/55%/ 50%	78%/78%/ 71%	102%/102%/ 93%	326%/326%/ 296%
Kofler and Clausen 2021 [48]	P	50 MW$_{th,LHV}$ / 64 MW$_{el}$	Straw	Pyrolysis	CFB	hot gas filter + "catalytic upgrading" + bio oil separation	("catalytic upgrading")	AEL	0.78	0.61	68%	53%	169%	76%
Giglio et al. 2021 [53]	P	7.4 MW$_{th,LHV}$ / 11.2 MW$_{el}$	woody biomass	Drying	CFB	-	-	SOEL	1.53	0.67	100%	75%	187%	124%

[a]: Scope: P: Process simulation, E: Estimation-based calculation approach
[b]: EFG: Entrained flow gasification, CFB: Circulating fluidized bed, FB: Fixed bed, TSG: Two-Stage gasifier (by Technical University of Denmark (DTU))
[c]: AEL: Alkaline electrolysis, SOEL: Solid oxide electrolysis, PEMEL: Proton exchange membrane electrolysis
[d]: DFB: dual fluidized bed indirect gasifier, SEG: dual fluidized bed sorption-enhanced gasifier

Table 5: Literature overview for Power-and-Biomass-to-MeOH studies including the scope, plant size, the used pretreatment, gasification, syngas cleaning, reforming, and electrolysis technologies. KPI values derived from the data in the respective literature.

Reference	Scope[a]	Plant Size[a]	Biomass Feedstock	Pretreatment	Gasifier[b]	Syngas cleaning	Reformer	Electrolyzer[c]	ER MW$_{el}$/MW$_{th}$	PY kg$_{MeOH}$/kg$_{db}$	η_C %	EY$_{PBIx}$ %	EY$_{BIx}$ %	EY$_{PIx}$ %
Oulette and Scott 1995 [2]	E	~2100 MW$_{th,LHV}$ / 2700 MWel	Wood chips or pyrolysed wood.		FB	AGR (not specified)	-	not specified	1.29	1.21	100%	57%	134%	100%
Specht et al. 1999 [3]	E	10 MW$_{th,LHV}$ / 14.7 MW$_{el}$	Wood chips	-	not specified	CO2 removal (not specified)	-	not specified	1.47	1.22	81%	51%	135%	82%
Mignard and Pritchard 2008 [4]	E	~31 MW$_{th,LHV}$ / 43 MW$_{el}$	Wood chips	-	FB	Washing and Drying (Techn. Not specified)	-	PME[d]	1.39	1.27	87%	54%	140%	88%
Hertwich and Zhang 2009 [8]	E	~370 MW$_{th,LHV}$ / 440 MW$_{el}$	Wood pellets	-	not specified	not specified cleaning technology + rWGS	not specified	not specified	1.19	1.21	90%	58%	134%	104%
Clausen et al. 2010 [12]	P	172 MW$_{th,LHV}$ / 111 MW$_{el}$	Wood chips	steam drying	CFB	Removal of particles (cyclone or filter), sulfur compnents (zinc oxide filter, COS hydrolysis or scrubber) and in some cases CO2 (amine scrubber)	-	AEL	0.64	1.10	88%	72%	122%	179%
Clausen 2011 [13]	P	2302 MW$_{th,LHV}$ / 2536 MW$_{el}$	Torrefied wood pellets	milling	EFG	(rWGS+)Removal of particles (cyclone or filter) + AGR (Rectisol + Guard beds)	-	AEL	1.10	1.27	97%	61%	140%	107%
Ridjan et al. 2013 [18]	E	not specified	not specified	not specified	not specified	not specified	-	SOEL	0.63	1.08	81%	74%	119%	193%
Hannula 2015 [21]	P	100 MW$_{th,LHV}$ / 35.4 MW$_{el}$	Forest residues chips	Belt drier	CFB	filter, sour WGS, water scrubber, AGR (MeOH/rectisol wash), guard beds	catalytic reformer	AEL	0.35	0.76	55%	58%	84%	185%
Clausen 2015 [20]	P	500 MW$_{th,LHV}$ /595 MW$_{el}$	Wood chips	steam drying + Torrefaction	EFG	rWGS, AGR(Rectisol)	-	AEL	1.19	1.21	96%	62%	134%	116%
Hannula 2016 [22]	P	100 MW$_{th,LHV}$/ 170 MW$_{el}$	Forest residues chips	Belt drier	CFB	filter , water scrubber, AGR (MeOH/Rectisol wash), guard beds	catalytic reformer	AEL	1.70	1.31	92%	58%	145%	98%
Trop and Goricanec 2016 [23]	P	600 MW$_{th,LHV}$ / 889.5 MW$_{el}$	Torrefied biomass	Mill Dryer	EFG	AGR (Selexol)	-	not specified	1.48	1.17	88%	52%	129%	87%
Firmansyah et al. 2018 [35]	E	25 MW$_{th,LHV}$ / 30 MW$_{el}$	Woody biomass	Drying	FB	Washing and Drying (Techn. Not specified)	-	AEL	1.19	1.14	85%	57%	126%	103%
Zhang et al. 2019 [43]	P	400 MW$_{th,LHV}$ /: 242 MW$_{el}$	Wood (sawdust)	-	EFG	Amine wash	-	SOEL	0.61	0.89	67%	60%	98%	153%
Butera et al. 2020 [47]	P	100 MW$_{th,LHV}$ / 41.8 MW$_{el}$	Straw	Pyrolysis	CFB	Guard bed, WGS, AGR (amine wash/MEA)	POX	SOEL	0.42	0.70	58%	58%	77%	228%
Butera et al. 2020 [49].	P	100 MW$_{th,LHV}$ / 89.2/83.7 MW$_{el}$	woody biomass	steam dryer + Milling	EFG	candle filter and sulfur removal (guard beds), + AGR (Rectisol) and optional WGS	-	SOEL	0.89/0.84	1.24/1.24	96%/97%	71%/74%	137%/137%	147%/161%
Zhang et al. 2020 [44]	P	65 MW$_{th,LHV}$ / 40 MW$_{el}$	woody biomass	-	EFG	AGR (MEA)	-	SOEL	0.61	0.89	66%	60%	98%	155%
Zhang et al. 2020 [45]	P	10 MW$_{th,LHV}$ / 8.5 MW$_{el}$	woody biomass	-	EFG	AGR (MEA)	-	SOEL	0.85	1.12	99%	63%	124%	127%
Poluzzi et al. 2020 [51]	P	not specified	woody biomass	Drying	CFB, DFB, SEG[e]	WGS + cleaning + AGR	ATR	not specified	0.39/0.39/0.39	0.73/0.73/0.67	55%/55%/50%	62%/62%/56%	81%/81%/74%	268%/268%/230%
Henning and Haase 2021 [54]	P	1177 MW$_{th,LHV}$/ 1175 MWel	Straw	Drying + Pyrolysis	EFG (slurry)	AGR (MEA)	-	AEL	1.00	0.97	78%	55%	108%	114%
Butera et al. 2021 [50]	P	100 MW$_{th,LHV}$/ 40 MW$_{el}$	woody biomass	steam dryer	TSG	candle filter + Cl + S removal (guard beds), + AGR (Amine wahs/MEA)	POX	SOEL	0.40	0.95	74%	74%	105%	248%
Kofler and Clausen 2021 [48]	P	50 MW$_{th,LHV}$/ 12 MW$_{el}$	wheat straw	Pyrolysis	CFB	hot gas filter + "catalytic upgrading" + bio oil separation	("catalytic upgrading")	AEL	0.24	f	f	f	-	-
Poluzzi et al. 2022 [52]	P	100 MW$_{th,LHV}$ / 129/67.5/63.3 MW$_{el}$	woody biomass	Belt dryer	CFB	Scrubber+LO-CAT (liquid redox)+guard bed	ATR	not specified	1.29/0.67/0.63	1.24/0.93/0.88	90%/68%/64%	61%/62%/61%	137%/103%/ 97%	110%/156%/164%
Melin et al. 2022 [113]	P	27.9 MW$_{th,LHV}$ / 43.5 MW$_{el}$	forest residues	Drying	CFB	Filter+Scrubber+Guard beds+Membrane separation	catalytic reformer	AEL	1.56	g	g	g	-	*
Fournas and Wei 2022 [56]	P	50 MW$_{th,LHV}$ / 56 MW$_{el}$	forest residues	Torrefaction	EFG	AGR (Rectisol)	-	PEMEL	1.12	1.24	92%	62%	137%	115%
Ostadi et al. 2023 [58]	P	197 MW$_{th,LHV}$ / 170 MW$_{el}$	woody biomass	drying, torrefaction, grinding	EFG	AGR (Selexol)	-	SOEL	0.86	1.30	94%	73%	144%	148%
Anetjärvi et al. 2023 [114]	P	54.6/79.6 MW$_{th,LHV}$ / 60.7/33.0 MW$_{el}$	woody biomass	Steam Drying	CFB	filtration + catalytic reforming + water scrubbing + AGR (Rectisol)	catalytic reformer	AEL	1.11/0.41	1.28/0.88	90%/62%	64%/66%	142%/97%	117%/205%

a: Scope: P: Process simulation, E: Estimation-based calculation approach (e.g. spreadsheet mass & energy balances). Plant size: Biomass input / Electrical power to electrolysis
b: EFG: Entrained flow gasification, CFB: Circulating fluidized bed, FB: Fixed bed, TSG: Two-Stage gasifier (by DTU)
c: AEL: Alkaline electrolysis, SOEL: Solid oxide electrolysis, PEMEL: Proton exchange membrane electrolysis
d: Pressure Module Electrolyzer
e: DFB: dual fluidized bed indirect gasifier, SEG: dual fluidized bed sorption-enhanced gasifier

f: DME as main product with MeOH as intermediate. PY: 0.33 $kg_{DME}/kg_{biomass,dry}$, DME-based η_C: 27%, DME-based EY: 32%. Not included in Figure 15 in main paper

g Ethanol as main product with MeOH as intermediate. PY: 0.952 $kg_{EtOH}/kg_{biomass,dry}$, Ethanol-based η_C: 91%, Ethanol-based EY: 53%. Not included in Figure 15 in main paper

Table 6: Literature overview for Power-and-Biomass-to-FT studies including the scope, plant size, the used pretreatment, gasification, syngas cleaning, reforming, and electrolysis technologies. KPI values derived from the data in the respective literature.

Reference	Scope[a]	Plant Size Biomass input / Electrical Power to electrolysis	Biomass Feedstock	Pretreatment	Gasifier[b]	Syngas cleaning	Reformer	Electrolyzer[c]	ER MW_{el}/MW_{th}	PY $kg_{FT}/kg_{biomass,dry}$	η_C %	EY %	EY$_{BtX}$ %	EY$_{PtX}$ %
Seiler et al. 2010 [11]	E	500 MW$_{th,LHV}$ / 535 MW$_{el}$	Torrefied wood	Hot air drying + torrefaction	EFG	Rectisol/Amine	not specified	not specified	1.07	0.50	100%	56%	117%	109%
Baliban et al. 2010 [10 d]	P	400 MW$_{th,LHV}$/ ~205 MW$_{el}$	Herbaceous biomass	Drying	CFB	rWGS, AGR(Rectisol)	ATR	not specified	0.51	0.48	100%	79%	d	d
Bernical et al. 2012 [16]	P	not specified	Lignocellulosic biomass	direct dryer + torrefaction + grinding	EFG	Chemical wash (amines) or Physical wash (methanol) (+WGS)	-	SOEL	0.84	0.36	61%	46%	84%	100%
Bernical et al. 2013 [17]	P	not specified	Woody biomass residues	direct dryer + torrefaction + grinding	EFG	Chemical wash (amines) or Physical wash (methanol) (+WGS)	steam reforming of tail gas	SOEL	0.87	0.37	62%	46%	86%	98%
Albrecht et al. 2017 [24]	P	109 MW$_{th,LHV}$ / 171 MW$_{el}$	Lignocellulosic biomass	Fast pyrolysis	EFG (slurry)	(r)WGS + Selexol wash	-	PEMEL	1.57	0.50	98%	47%	117%	79%
Hillestad et al. 2018 [37]	P	435 MW$_{th,LHV}$ / 415 MW$_{el}$	Wood chips	Steam drying + torrefaction + grinding	EFG	(rWGS), Selexol wash	-	SOEL	0.95	0.50	91%	65%	118%	148%
Kurkela 2019 [42 a]	E	23 MW$_{th,LHV}$ / 27 MW$_{el}$	Woody biomass	Drying	FB	hot filtration + guard beds	catalytic reformer	not specified	1.17	0.49	85%	54%	115%	102%
Zhang et al. 2020 [45]	P	10 MW$_{th,LHV}$ / 4.9 MW$_{el}$	woody biomass	-	EFG	-	-	SOEL	0.49	0.34	62%	50%	78%	138%
Habermeyer et al. 2021 [55]	P	200 MW$_{th,LHV}$ / 187.9 MW$_{el}$	Forest residue chips	Drying	CFB	hot gas filter, Selexol scrubber, ZnO guard bed	ATR	AEL	0.94	0.38	61%	50%	89%	112%
Dossow et al. 2021 [46]	P	200 MW$_{th,LHV}$ / PEM: 150/220/320 MW$_{el}$ SOEL: 120/180/260 MW$_{el}$	Woddy biomass residues	Drying + torrefaction + grinding	EFG	sour WGS + hot gas cleaning	-	PEMEL SOEL	1.6/1.1/0.75 1.3/0.9/0.6	0.57/0.47/0.40 0.57/0.47/0.40	97%/79%/67% 97%/79%/67%	47%/47%/47% 53%/53%/53%	134%/109%/93%/ 134%/109%/93%	72%/83%/95% 88%/103%/124%
Pandey et al. 2022 [57]	P	50 MW$_{th,LHV}$ / 52/35.5/51/40 MW$_{el}$	wood chips	Steam drying + torrefaction + grinding	EFG	rWGS, Selexol scrubber, guard bed	-	SOEL	1.04/0.71/1.02/ 0.8	0.56/0.53/0.55/ 0.50	96%/91%/96%/ 86%	62%/70%/62%/ 62%	130%/123%/ 129%/116%	119%/162%/119%/13 4%
Habermeyer et al. 2023 [115]	P	50 MW$_{th,LHV}$ / 42/31.3/58.3/31.4/54.6 MW$_{el}$	Forest residues Agriculture residues	Drying	FB	adsorption-based gas cleaning	Tar reformer	AEL SOEL	0.84/0.63/1.17/ 1.09 0.63	0.35/0.20/0.40/ 0.35 0.35	60%/34%/69%/ 57% 60%	53%/34%/51%/ 46% 59%	82%/d/94%/82 %	147%/ d/113%/217% 107%

a: Scope: P: Process simulation, E: Estimation-based calculation approach
b: EFG: Entrained flow gasification, CFB: Circulating fluidized bed, FB: Fixed bed
c: AEL: Alkaline electrolysis, SOEL: Solid oxide electrolysis, PEMEL: Proton exchange membrane electrolysis
d: excluded in graphs due to implausibility of KPIs

Table 7: Literature overview for PBtX process simulation studies using parallel co-electrolysis (SOEL: Solid oxide electrolysis) and entrained flow gasification (EFG) including the plant size, the used pretreatment, gasification, syngas cleaning, reforming, and electrolysis technologies. KPI values derived from the data in the respective literature.

Reference	Plant Size[a]	Main product	Biomass Feedstock	Pretreatment	Gasifier	Syngas cleaning	Reformer	ER MW$_{el}$/MW$_{th}$	PY Kg$_{fuel}$/kg$_{db}$	η_C %	EY$_{PBtX}$ %	EY$_{BtX}$ %	EY$_{PtX}$ %
Zhang et al. 2020 [45]	10 MW$_{th,LHV}$/13.3 MW$_{el}$ 10 MW$_{th,LHV}$/8.7 MW$_{el}$ 10 MW$_{th,LHV}$/6.9 MW$_{el}$	SNG MeOH FT	Woody biomass.	Not specified	EFG	Not specified	-	1.33 0.87 0.69	0.51 kg$_{SNG}$/kg$_{db}$ 1.00 kg$_{MeOH}$/kg$_{db}$ 0.35 kg$_{FT}$/kg$_{db}$	75% 75% 60%	63% 61% 50%	142% 111% 80.7%	113% 136% 131%
Steinrücken et al. 2023 [116]	200 MW$_{th,LHV}$/117.5 MW$_{el}$ 200 MW$_{th,LHV}$/138.5 MW$_{el}$ 200 MW$_{th,LHV}$/148.9 MW$_{el}$ 200 MW$_{th,LHV}$/165.1 MW$_{el}$	FT	Woddy biomass residues	Drying + torrefaction + grinding	EFG	sour WGS + hot gas cleaning	-	0.59 0.69 0.74 0.83	0.50 kg$_{FT}$/ kg$_{db}$ 0.53 kg$_{FT}$/ kg$_{db}$ 0.54 kg$_{FT}$/ kg$_{db}$ 0.56 kg$_{FT}$/ kg$_{db}$	84% 89% 92% 94%	64% 65% 64% 63%	116% 123% 126% 130%	145% 137% 130% 124%

[a]:Plant size: Biomass input / Electrical power to electrolysis

Table 8: Literature overview for process simulation studies of in-line integration of co-electrolysis into BtX processes (eBtX) including the used gasification technologies. KPI values derived from the data in the respective literature.

Reference	Plant Size[a]	Main Product	Biomass Feedstock	Pretreatment	Gasifier[a]	Syngas cleaning	Reformer	ER MW$_{el}$/MW$_{th}$	PY kg$_{product}$/kg$_{biomass,dry}$	η_C %	EY %	EY$_{BtX}$ %	EY$_{PtX}$ %
Pozzo et al. 2015 [117]	1 MW$_{th,LHV}$/0.81 MW$_{el}$	DME	Woody biomass	Steam drier	TSG	filter, cyclone, wet scrubber, AGR	-	0.81	0.86 kg$_{DME}$/kg$_{biomass,dry}$	91%	75%	138%	165%
Monaco et al. 2018 [118]	18 MW$_{th,LHV}$/13.7 MW$_{el}$ 18 MW$_{th,LHV}$/18.9 MW$_{el}$ 18 MW$_{th,LHV}$/10.2 MW$_{el}$	DME SNG FT	residual biomass	-	TSG (3)	-	-	0.76 1.05 0.57	0.86 kg$_{DME}$/kg$_{biomass,dry}$ 0.59 kg$_{SNG}$/kg$_{biomass,dry}$ 0.46 kg$_{FT}$/kg$_{biomass,dry}$	90% 89% 80%	78% 80% 71%	139% 164% 107%	181% 156% 207%
Clausen et al. 2019 [119]	100 MW$_{th,LHV}$/113.7 MW$_{el}$	SNG	Wood pellets	-	TSG[b]	particle removal + sulfur guard	POX	1.14	0.65 kg$_{SNG}$/kg$_{biomass,dry}$	99%	82%	181%	149%
Clausen et al. 2019 [120]	51.5 MW$_{th,LHV}$/37.7 MW$_{el}$ 51.5 MW$_{th,LHV}$/35 MW$_{el}$	SNG	Manure (biogas plant) Manure (pre-processed)	Steam drier	TSG[c] (2)[d]	particle removal + sulfur guard	POX	0.71 0.65	0.51 kg$_{SNG}$/kg$_{biomass,dry}$ 0.42 kg$_{SNG}$/kg$_{biomass,dry}$	54% 44%	81% 65%	143% 116%	185% 148%
Butera et al. 2019 [e] [121]	100 MW$_{th,LHV}$/33.5 MW$_{el}$+11.7MW$_{th}$	MeOH	Wood chips	Steam drier	TSEG	particle removal + sulfur guard + AGR (MEA)	pre-reformer	0.45	1.02 kg$_{MeOH}$/kg$_{biomass,dry}$	76%	77%	113%	240%
Butera et al. 2020 [e] [122]	100 MW$_{th,LHV}$/55.3 MW$_{el}$+12.5MW$_{th}$	MeOH	Wood chips	Steam drier	TSEG	candle filter and sulfur removal (guard beds), + AGR (Amine wash/MEA)	pre-reformer	0.68	1.19 kg$_{MeOH}$/kg$_{biomass,dry}$	89%	77%	131%	186%
Butera et al. 2020 [e] [49]	100 MW$_{th,LHV}$/55.3 MW$_{el}$+11.3MW$_{th}$ 100 MW$_{th,LHV}$/55.3 MW$_{el}$+18.5MW$_{th}$ 100 MW$_{th,LHV}$/52.3 MW$_{el}$+3.5MW$_{th}$	MeOH	woody biomass	steam dryer	TSEG TSEHG e-BFB	candle filter and sulfur removal (guard beds), + AGR (Amine wash/MEA)	pre-reformer - SMR	0.67 0.74 0.72	1.19 kg$_{MeOH}$/kg$_{biomass,dry}$ 1.20 kg$_{MeOH}$/kg$_{biomass,dry}$ 1.10 kg$_{MeOH}$/kg$_{biomass,dry}$	89% 90% 82%	77% 75% 70%	131% 133% 121%	189% 174% 163%
Steinrücken et al. 2023 [116]	200 MW$_{th,LHV}$/63 MW$_{el}$ 200 MW$_{th,LHV}$/114.4 MW$_{el}$ 200 MW$_{th,LHV}$/136.4 MW$_{el}$	FT	Woddy biomass residues	Drying + torrefaction + grinding	EFG	sour WGS + hot gas cleaning	-	0.32 0.57 0.68	0.36 kg$_{FT}$/kg$_{biomass,dry}$ 0.44 kg$_{FT}$/kg$_{biomass,dry}$ 0.47 kg$_{FT}$/kg$_{biomass,dry}$	61% 74% 79%	57% 58% 58%	84.0% 103% 110%	177% 133% 123%

[a]: Plant size: Biomass input / el. power to electrolysis + el. power to el. heated gasifier (LHV$_{DME}$ = 28.9 MJ/kg, LHV$_{Biomass}$ = 18 MJ/kg). TSG: Two-Stage gasifier (by DTU); TSEG: two-stage electro-gasifier, gasifier is electrically-heated with heating elements in the bed; TSEHG: two-stage electrically-heated gasifier, gas to gasifier is electrically preheated, e-BFB: bubbling fluidized bed gasifier heated via heat pipes; EFG: Entrained flow gasification
[b] new TSG design using two updraft fixed beds, one for pyrolysis and one for char gasification
[c] new TSG design using updraft fixed pyrolysis and fluid bed char gasification
[d]: case 1: biogas plant integrated, case 2: pre-processed manure as feedstock
[e]: in addition to co-electrolysis, electricity is used to heat gasifier. EY includes SOEL and el. heating requirements

3. GHG emission calculation

This section contains the calculations of GHG emissions for the transportation of biomass (Section 3.1) and for the supply of electricity (Section 0).

3.1. Transportation of biomass

This section presents the assumptions and results presented in Section 7.1.2. in the main paper. Table 9 shows the assumptions for the calculations.

Table 9: Values and assumptions used for the calculation.

	Value	Unit	Comment
Lower heating value MeOH	19.9	MJ/kg	-
Molar mass MeOH	32.04	g/mol	-
Molar mass Carbon	12.01	g/mol	-
Plant capacity	100	$MW_{th,LHV}$	Own assumption
Full load hours	8000	h	Own assumption
Biomass harvest density	56.0	$t_{BM,wet}$/km² a	Calculated with 224 Mt/a of biomass residues [123] and a land area of the European Union of 4.00 Mio km² [124]
Residual biomass moisture content	30	wt%	Own assumption
Carbon content biomass	50	wt%	Own assumption
Truck load capacity	30	$t_{BM,wet}$	Own assumption
CO_2 emissions of truck transport	0.81	kg CO_2/km	Calculated with a fuel consumption of 30 l/100 km and an emission factor for diesel of 2.7 kg CO_2/l [125]

The process was scaled to a constant output of methanol. The carbon efficiency of the process was altered from 40 to 90 % to account for different degrees of electrification. Based on the altered carbon efficiency, the biomass demand changes. Since the biomass supply area is assumed to be a circle around the plant, the biomass demand leads to a maximum radius to cover the demand for the plant. To calculate the transport distance of biomass, the mean radius $\bar{r}$ for transportation weighted by the area is calculated according to the following equation:

$$\bar{r} = \frac{1}{A_0} \int_0^{r_0} r\, dA = \frac{1}{\pi r_0^2} \int_0^{r_0} 2\pi r^2 dr = \frac{2}{r_0^2} \frac{1}{3} r_0^3 = \frac{2}{3} r_0$$

Based on this mean radius which is the mean distance that biomass has to travel to reach the plant, the yearly number of truck trips can be calculated and consequently the amount of traveled kilometers per year. With the fuel consumption, the annual CO_2 emissions can be calculated. Figure 4 shows the required radius, land area, and GHG emissions over carbon efficiency. The results as values are shown in

Table 10. The ER shown in graphs is derived from the relationship between carbon efficiency and ER as shown in Equation (7) using $\overline{EY}_{PtX,LT}$, $\overline{EY}_{PtX,HT}$ and $\overline{EY}_{PtX,co-electrolysis}$ from Table 1.

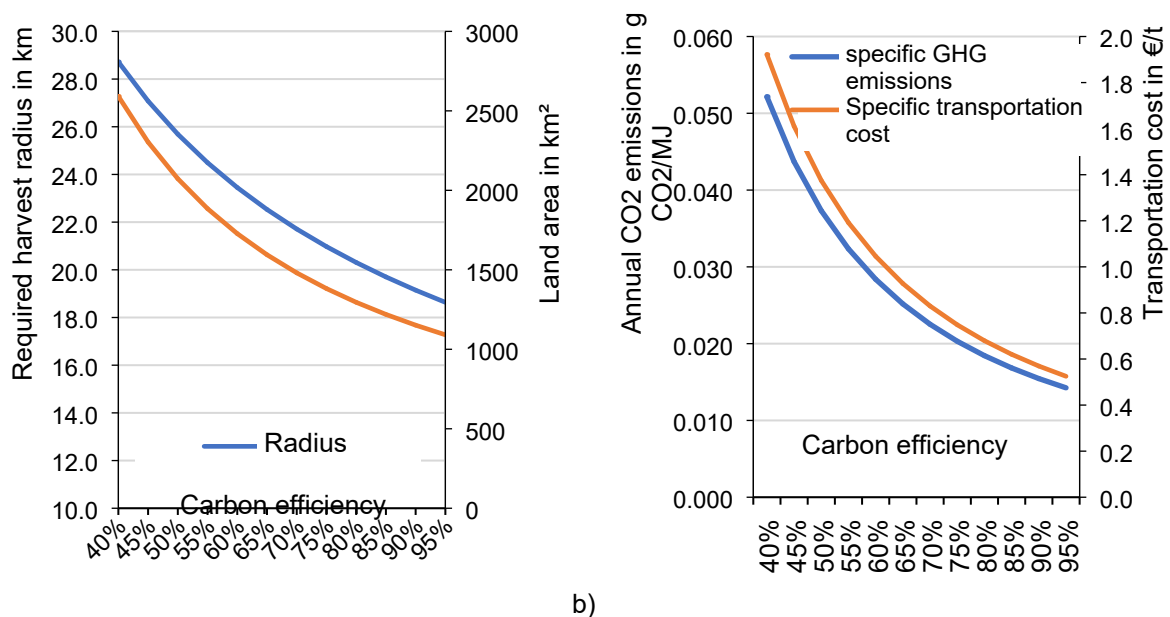a)   b)

Figure 4: Influence of carbon efficiency (degree of electrification) on a) required harvest radius and land area, b) GHG emissions associated with biomass transportation and transportation cost.

Table 10: Results for transport distance calculation and GHG emissions

Carbon efficiency	Annual biomass demand wet in $t_{BM,wet}$/a	Required land area in km^2	Radius in km	Mean radius in km	Annual distance travelled in km	Specific CO_2 emissions in g CO_2/MJ_{MeOH}
40%	145,249	2,591	28.7	19.1	185,406	0.052
45%	129,110	2,303	27.1	18.1	155,380	0.044
50%	116,199	2,073	25.7	17.1	132,666	0.037
55%	105,635	1,885	24.5	16.3	114,993	0.032
60%	96,832	1,728	23.5	15.6	100,922	0.028
65%	89,384	1,595	22.5	15.0	89,504	0.025
70%	82,999	1,481	21.7	14.5	80,088	0.023
75%	77,466	1,382	21.0	14.0	72,214	0.020
80%	72,624	1,296	20.3	13.5	65,551	0.018
85%	68,352	1,219	19.7	13.1	59,853	0.017
90%	64,555	1,152	19.1	12.8	54,935	0.015

3.2. Indirect process emissions from electricity generation

The assumptions and calculations presented here are the basis for Figure 18 in Section 7.1.2. The used emission factors for electricity shown in the Figure are presented in Table 11.

$$\eta_C(EY_{PtX} \; ER_{PBtX,LT} = 1.3, \; ER_{PBtX,HT} = 1.0, ER_{P-/eBtX,co-electrolysis} = 0.9) = 90\%_1$$

$$EY_{PtX,SNG,min} = 1.06 \; MW_{SNG} \; MW_{el.}^{-1} \; \textit{ER=1.3} \; MW_{el.} \; MW_{biomass}^{-1}$$

$$EY_{PtX,SNG,max} = 1.56 \; MW_{SNG} \; MW_{el.}^{-1} \; \textit{ER=1.1} \; MW_{el.} \; MW_{biomass}^{-1}$$

$$EY_{PtX,MeOH,min} = 1.11 \; MW_{MeOH} \; MW_{el.}^{-1} \; \textit{ER=1.2} \; MW_{el.} \; MW_{biomass}^{-1}$$

$$EY_{PtX,MeOH,max} = 1.83 \; MW_{MeOH} \; MW_{el.}^{-1} \; \textit{ER=0.7} \; MW_{el.} \; MW_{biomass}^{-1}$$

$$EY_{PtX,FT,min} = 0.85 \; MW_{G} \; MW_{el.}^{-1} \; \textit{ER=1.2} \; MW_{el.} \; MW_{biomass}^{-1}$$

$$EY_{PtX,FT,max} = 1.33 \; MW_{FT} \; MW_{el.}^{-1} \; \textit{ER=0.7} \; MW_{el.} \; MW_{biomass}^{-1}$$

$$EY_{PtX} = 0.55 \; MW_{H2} \; MW_{el.}^{-1}$$

$$EY_{BtX,SNG} = 1.56 \; MW_{SNG} \; MW_{el.}^{-1} \; \textit{ER=1.1} \; MW_{el.} \; MW_{biomass}^{-1}$$

$$EY_{BtX,MeOH} = 1.11 \; MW_{MeOH} \; MW_{el.}^{-1} \; \textit{ER=1.2} \; MW_{el.} \; MW_{biomass}^{-1}$$

$$EY_{BtX,FT} = 0.85 \; MW_{G} \; MW_{el.}^{-1} \; \textit{ER=1.2} \; MW_{el.} \; MW_{biomass}^{-1}$$

As reference, the emissions of conventional fossil fuels are used:

specific emissions natural gas: 55.8 g CO_2/MJ [126]

specific emissions natural gas derived methanol: 110.0 g CO_2/MJ [127]

specific emissions Gas-to-FT: 86.2 g CO_2/MJ [128]

Table 11. Emission factors of electricity [129]

Country	Electricity emission factor in g CO_2/kWh$_{el}$
Norway	4.5
Canada	110.8
Brazil	129.5
UK	193.4
Germany/USA	377.6

---

[1] $ER_{PBtX,LT} = 1.3, \; ER_{PBtX,HT} = 1.0, ER_{P-/eBtX,co-electrolysis} = 0.9$

Japan	461.5
China	557.2

4. Potential of e/PBtX

The calculations of the methanol production potential are based on the data supplied in Table 12. The results are reported in the paper in section "7.1.2 Land use and greenhouse gas emissions". With the annual residual biomass potential and the water content it is possible to calculate the annual production of methanol via BtX or e-/PBtX with the product yield.

Table 12. Reference values for the calculation of the potential of BtX and PBtX

	Unit	Value	Ref.	Comment
Annual residual biomass potential in Europe (wet)	Mt/a	224	[123]	The biomass potential is based on crop residues, forestry residues, fractions of the municipal solid waste and used cooking oil.
Residual biomass moisture content	wt%	30	-	Own assumption
Global methanol demand	Mt/a	105.8	[130]	In 2022
Product yield BtMeOH	$t_{MeOH}/t_{biomass,dry}$	0.53	[105]	-
Product yield P-/eBtMeOH	$t_{MeOH}/t_{biomass,dry}$	1.2	-	[a]

[a] $PY_{P-/eBtX} = \eta_C \cdot \dfrac{w_{C,biomass,dry}}{w_{C,product}} = 90\% \cdot \dfrac{w_{C,biomass,dry}}{w_{C,product}}$. On a dry and ash-free basis a carbon content of 50wt.% is used.

With $w_{C,MeOH} = 0.375 \; kg_C \; kg_{MeOH}^{-1}$; $PY_{max} = 0.9 \cdot \dfrac{0.5 \; kg_C \; kg_{BM,dry}^{-1}}{0.375 \; kg_C \; kg_{MeOH}^{-1}}$

5. References

1 M. A. Dietenberger and M. Anderson, *Ind. Eng. Chem. Res.*, 2007, **46**, 8863–8874.

2 N. Oulette, H.-H. Rogner and D. S. Scott, *International Journal of Hydrogen Energy*, 1995, **20**, 873–880.

3 M. Specht, A. Bandi, F. Baumgart, C. N. Murray and J. Gretz, in *Greenhouse Gas Control Technologies 4*, Elsevier, 1999, Vol. 20, pp. 723–727.

4 D. Mignard and C. Pritchard, *Chemical Engineering Research and Design*, 2008, **86**, 473–487.

5 M. Gassner and F. Maréchal, *Energy*, 2008, **33**, 189–198.

6 R. Agrawal and N. R. Singh, *AIChE J.*, 2009, **55**, 1898–1905.

7 R. Agrawal, N. R. Singh, F. H. Ribeiro, W. N. Delgass, D. F. Perkis and W. E. Tyner, *Computers & Chemical Engineering*, 2009, **33**, 2012–2017.

8 E. G. Hertwich and X. Zhang, *Environmental science & technology*, 2009, **43**, 4207–4212.

9 R. Agrawal and N. R. Singh, *Annual review of chemical and biomolecular engineering*, 2010, **1**, 343–364.

10 R. C. Baliban, J. A. Elia and C. A. Floudas, *Ind. Eng. Chem. Res.*, 2010, **49**, 7343–7370.

11 J.-M. Seiler, C. Hohwiller, J. Imbach and J.-F. Luciani, *Energy*, 2010, **35**, 3587–3592.

12 L. R. Clausen, N. Houbak and B. Elmegaard, *Energy*, 2010, **35**, 2338–2347.

13 L. Røngaard Clausen, *Design of novel DME/methanol synthesis plants based on gasification of biomass. Dissertation*, DTU Mechanical Engineering; DCAMM, Lyngby, 1st edn., 2011, No. S 123.

14 R. Agrawal and D. S. Mallapragada, *AIChE J.*, 2010, **56**, 2762–2768.

15 D. S. Mallapragada, N. R. Singh and R. Agrawal, in *21st European Symposium on Computer Aided Process Engineering*, Elsevier, Amsterdam, 1st edn., 2011, vol. 29, pp. 1889–1893.

16 Q. Bernical, X. Joulia, I. Noirot-Le Borgne, P. Floquet, P. Baurens and G. Boissonnet, in *11th international symposium on process systems engineering - PSE2012*, Elsevier, Oxford, 2012, vol. 31, pp. 865–869.

17 Q. Bernical, X. Joulia, I. Noirot-Le Borgne, P. Floquet, P. Baurens and G. Boissonnet, *Ind. Eng. Chem. Res.*, 2013, **52**, 7189–7195.

18 I. Ridjan, B. Vad Mathiesen and D. Connolly, *SOEC pathways for the production of synthetic fuels. The transport case*, Department of Development and Planning, Aalborg University, 2013.

19 L. R. Clausen, *Energy*, 2014, **77**, 597–607.

20 L. R. Clausen, *Energy*, 2015, **85**, 94–104.

21 I. Hannula, *Biomass and Bioenergy*, 2015, **74**, 26–46.

22 I. Hannula, *Energy*, 2016, **104**, 199–212.

23 P. Trop and D. Goricanec, *Energy*, 2016, **108**, 155–161.

24 F. G. Albrecht, D. H. König, N. Baucks and R.-U. Dietrich, *Fuel*, 2017, **194**, 511–526.

25 R.-U. Dietrich, F. G. Albrecht, S. Maier, D. H. König, S. Estelmann, S. Adelung, Z. Bealu and A. Seitz, *Biomass and Bioenergy*, 2018, **111**, 165–173.

26 D. H. König, F. G. Albrecht and R.-U. Dietrich, *Power and Biomass-to-Liquid (PBtL): a Promising Approach to Produce Biofuels using Electricity*, 2016.

27 P. Nikparsa, R. Rauch and A. A. Mirzaei, *Monatsh Chem*, 2017, **148**, 1877–1886.

28 K. Koponen and I. Hannula, *Applied Energy*, 2017, **200**, 106–118.

29 K. Onarheim, I. Hannula and Y. Solantausta, *Energy*, 2020, **199**, 117337.

30 L. R. Clausen, *Energy*, 2017, **125**, 327–336.

31 U. Henriksen, J. Ahrenfeldt, T. K. Jensen, B. Gøbel, J. D. Bentzen, C. Hindsgaul and L. H. Sørensen, *0360-5442*, 2006, **31**, 1542–1553.

32 L. R. Clausen, B. Elmegaard, J. Ahrenfeldt and U. Henriksen, *Energy*, 2011, **36**, 5805–5814.

33 J. Ahrenfeldt, U. Henriksen, T. K. Jensen, B. Gøbel, L. Wiese, A. Kather and H. Egsgaard, *Energy Fuels*, 2006, **20**, 2672–2680.

34 H. Æ. Sigurjonsson and L. R. Clausen, *Applied Energy*, 2018, **216**, 323–337.

35 H. Firmansyah, Y. Tan and J. Yan, *Energy Procedia*, 2018, **145**, 576–581.

36 R. Anghilante, C. Müller, M. Schmid, D. Colomar, F. Ortloff, R. Spörl, A. Brisse and F. Graf, *Energy Conversion and Management*, 2019, **183**, 462–473.

37 M. Hillestad, M. Ostadi, G. Alamo Serrano, E. Rytter, B. Austbø, J. G. Pharoah and O. S. Burheim, *Fuel*, 2018, **234**, 1431–1451.

38 Ostadi Mohammad, Austbo Bjorn and Hillestad Magne, *Chemical Engineering Transactions*, 2019, **76**, 205–210.

39 M. Ostadi, E. Rytter and M. Hillestad, *Biomass and Bioenergy*, 2019, **127,** https://www.scopus.com/inward/record.uri?eid=2-s2.0-85067668213&doi=10.1016%2fj.biombioe.2019.105282&partnerID=40&md5=1723faf52ef6aaf79829932e8bbdbd7e.

40 M. Ostadi, B. Austbø and M. Hillestad, in *Computer Aided Chemical Engineering : Proceedings of the 9 International Conference on Foundations of Computer-Aided Process Design*, ed. S. G. Muñoz, C. D. Laird and M. J. Realff, Elsevier, 2019, vol. 47, pp. 287–292.

41 A. S. Nielsen, M. Ostadi, B. Austbø, M. Hillestad, G. del Alamo and O. Burheim, *Fuel*, 2022, **321**, 123987.

42 E. Kurkela, S. Tuomi, M. Kurkela and I. Hiltunen, *Flexible Hybrid Process for Combined Production of Heat, Power and Renewable Feedstock for Refineries*, 2019.

43 H. Zhang, L. Wang, F. Maréchal and U. Desideri, *Development of Integrated High Temperature and Low Temperature Fischer-Tropsch System for High Value Chemicals Coproduction*, 2019, **158**, 4548–4553.

44 H. Zhang, L. Wang, M. Pérez-Fortes, J. van Herle, F. Maréchal and U. Desideri, *Applied Energy*, 2020, **258**, 114071.

45 H. Zhang, L. Wang, J. van Herle, F. Maréchal and U. Desideri, *Applied Energy*, 2020, **270**, 115113.

46 M. Dossow, V. Dieterich, A. Hanel, H. Spliethoff and S. Fendt, *Renewable and Sustainable Energy Reviews*, 2021, **2021**.

47 G. Butera, R. Ø. Gadsbøll, G. Ravenni, J. Ahrenfeldt, U. B. Henriksen and L. R. Clausen, *Energy*, 2020, **199**, 117405.

48 R. Kofler and L. R. Clausen, *Smart Energy*, 2021, **2**, 100015.

49 G. Butera, S. Fendt, S. H. Jensen, J. Ahrenfeldt and L. R. Clausen, *Energy*, 2020, **208**, 118432.

50 G. Butera, S. H. Jensen, J. Ahrenfeldt and L. R. Clausen, *Fuel Processing Technology*, 2021, **215**, 106718.

51 A. Poluzzi, G. Guandalini and M. C. Romano, *Biomass and Bioenergy*, 2020, **142**, 105618.

52 A. Poluzzi, G. Guandalini, S. Guffanti, M. Martinelli, S. Moioli, P. Huttenhuis, G. Rexwinkel, J. Palonen, E. Martelli, G. Groppi and M. C. Romano, *Front. Energy Res.*, 2022, **9**.

53 E. Giglio, G. Vitale, A. Lanzini and M. Santarelli, *Biomass and Bioenergy*, 2021, **148**, 106017.

54 M. Hennig and M. Haase, *Fuel Processing Technology*, 2021, **216**, 106776.

55 F. Habermeyer, E. Kurkela, S. Maier and R.-U. Dietrich, *Front. Energy Res.*, 2021, 684.

56 N. de Fournas and M. Wei, *Energy Conversion and Management*, 2022, **257**, 115440.

57 U. Pandey, K. R. Putta, K. R. Rout, E. Rytter, E. A. Blekkan and M. Hillestad, *Front. Energy Res.*, 2022, **10**.

58 M. Ostadi, L. Bromberg, D. R. Cohn and E. Gençer, *Fuel*, 2023, **334**, 126697.

59 S. Stenström, *Drying Technology*, 2020, **38**, 825–845.

60 A. S. Mujumdar, *Handbook of Industrial Drying*, CRC Press, 2020.

61 Micronex Systems Inc, *Infrared Drying Conveyor,* available at: https://micronexsystems.com/infrared-drying-conveyor/, accessed 22 July 2022.

62 A. Motevali, S. Minaei and M. H. Khoshtagaza, *Energy Conversion and Management*, 2011, **52**, 1192–1199.

63 S. Bhattarai, J.-H. Oh, Y. S. Choi, K. C. Oh, S. H. Euh and D. H. Kim, *Journal of Biosystems Engineering*, 2012, **37**, 385–397.

64 H. S. EL-Mesery and S. E. El-khawaga, *Case Studies in Thermal Engineering*, 2022, **33**, 101953.

65 J. Yi, X. Li, J. He and X. Duan, *Drying Technology*, 2020, **38**, 2039–2054.

66 P. Rattanadecho and N. Makul, *Drying Technology*, 2016, **34**, 1–38.

67 A. A. Arpia, W.-H. Chen, S. S. Lam, P. Rousset and M. D. G. de Luna, *Chemical Engineering Journal*, 2021, **403**, 126233.

68 M. Amer, M. Nour, M. Ahmed, I. El-Sharkawy, S. Ookawara, S. Nada and A. Elwardany, *Biomass Conv. Bioref.*, 2021, **11**, 2855–2868.

69 M. Amer, M. Nour, M. Ahmed, S. Ookawara, S. Nada and A. Elwardany, *Bioresource technology*, 2019, **286**, 121400.

70 X. Wang, H. Chen, K. Luo, J. Shao and H. Yang, *Energy Fuels*, 2008, **22**, 67–74.

71 H. Liu, J. E, X. Ma and C. Xie, *Drying Technology*, 2016, **34**, 1397–1405.

72 Y. Xue, C. Wang, Z. Hu, Y. Zhou, G. Liu, H. Hou, Y. Xiao, T. Wang and J. Li, *Waste management (New York, N.Y.)*, 2018, **78**, 917–928.

73 M. A. H. Mohd Fuad, M. F. Hasan and F. N. Ani, *Fuel*, 2019, **253**, 512–526.

74 S.-H. Ho, C. Zhang, W.-H. Chen, Y. Shen and J.-S. Chang, *Bioresource technology*, 2018, **264**, 7–16.

75 B. Yan, L. Jiao, J. Li, X. Zhu, S. Ahmed and G. Chen, *Energy*, 2021, **220**, 119794.

76 F. Jin, *Application of Hydrothermal Reactions to Biomass Conversion*, Springer Berlin Heidelberg, Berlin, Heidelberg, 2014.

77 S. Nizamuddin, H. A. Baloch, M. T. H. Siddiqui, N. M. Mubarak, M. M. Tunio, A. W. Bhutto, A. S. Jatoi, G. J. Griffin and M. P. Srinivasan, *Rev Environ Sci Biotechnol*, 2018, **17**, 813–837.

78 S. E. Elaigwu and G. M. Greenway, *Fuel Processing Technology*, 2016, **149**, 305–312.

79 S. E. Elaigwu and G. M. Greenway, *Journal of Analytical and Applied Pyrolysis*, 2016, **118**, 1–8.

80 J. Zhang, Y. An, A. Borrion, W. He, N. Wang, Y. Chen and G. Li, *Bioresource technology*, 2018, **259**, 91–98.

81 M. F. Zulkornain, A. H. Shamsuddin, S. Normanbhay, J. Md Saad, Y. S. Zhang, S. Samsuri and W. A. Wan Ab Karim Ghani, *Carbon Capture Science & Technology*, 2021, **1**, 100014.

82 Y. Shao, H. Tan, D. Shen, Y. Zhou, Z. Jin, D. Zhou, W. Lu and Y. Long, *Fuel*, 2020, **266**, 117146.

83 L. Briesemeister, M. Kremling, S. Fendt and H. Spliethoff, *Chem. Eng. Technol.*, 2017, **40**, 270–277.

84 D. J. Lane, E. Truong, F. Larizza, P. Chiew, R. de Nys and P. J. van Eyk, *Energy Fuels*, 2018, **32**, 4149–4159.

85 X. Zhuang, Y. Song, H. Zhan, X. Yin and C. Wu, *Fuel*, 2020, **260**, 116320.

86 S. M. Heilmann, H. T. Davis, L. R. Jader, P. A. Lefebvre, M. J. Sadowsky, F. J. Schendel, M. G. von Keitz and K. J. Valentas, *Biomass and Bioenergy*, 2010, **34**, 875–882.

87 A. Sarvaramini and F. Larachi, *Fuel*, 2014, **116**, 158–167.

88 A. Sarvaramini, G. P. Assima and F. Larachi, *Chemical Engineering Journal*, 2013, **229**, 498–507.

89 F. Yang, Q. Yu, W. Duan, Z. Qi and Q. Qin, *Catalysis Communications*, 2021, **150**, 106261.

90 F. Yang, Q. Yu, W. Duan, Z. Qi and Q. Qin, *ACS omega*, 2021, **6**, 31026–31036.

91 T. M. Ismail, K. Yoshikawa, T. Kobori, Y. Kobayashi, K. Kanazawa, F. Takahashi and M. Abd El-Salam, *Applied Energy*, 2022, **311**, 118554.

92 E. Calcio Gaudino, G. Cravotto, M. Manzoli and S. Tabasso, *Green Chem.*, 2019, **21**, 1202–1235.

93 M. B. Gawande, S. N. Shelke, R. Zboril and R. S. Varma, *Accounts of chemical research*, 2014, **47**, 1338–1348.

94 A. Jha, in *Nanofibers. Synthesis, Properties and Applications*, ed. B. Kumar, IntechOpen, Erscheinungsort nicht ermittelbar, 2021.

95 H. Will, P. Scholz and B. Ondruschka, *Chem. Eng. Technol.*, 2004, **27**, 113–122.

96 H. M. Nguyen, J. Sunarso, C. Li, G. H. Pham, C. Phan and S. Liu, *Applied Catalysis A: General*, 2020, **599**, 117620.

97   T. Durka, T. van Gerven and A. Stankiewicz, *Chem. Eng. Technol.*, 2009, **32**, 1301–1312.

98   A. Stankiewicz, F. E. Sarabi, A. Baubaid, P. Yan and H. Nigar, *Chemical record (New York, N.Y.)*, 2019, **19**, 40–50.

99   M. Jouny, G. S. Hutchings and F. Jiao, *Nat Catal*, 2019, **2**, 1062–1070.

100   D. Klüh, H. Nieminen, K. Melin, A. Laari and T. Koiranen, *Front. Energy Res.*, 2023, **11**.

101   H. M. Fruehauf, F. Enzmann, F. Harnisch, R. Ulber and D. Holtmann, *Biotechnology journal*, 2020, **15**, e2000066.

102   L. Jourdin, J. Sousa, N. van Stralen and D. P. Strik, *Applied Energy*, 2020, **279**, 115775.

103   S. Ghosh, S. Gupta, M. Gregoire, T. Ourlin, P.-F. Fazzini, E. Abi-Aad, C. Poupin and B. Chaudret, *Nanomaterials (Basel, Switzerland)*, 2023, **13**.

104   W. Wang, G. Tuci, C. Duong-Viet, Y. Liu, A. Rossin, L. Luconi, J.-M. Nhut, L. Nguyen-Dinh, C. Pham-Huu and G. Giambastiani, *ACS Catal.*, 2019, **9**, 7921–7935.

105   A. Hanel, V. Dieterich, S. Bastek, H. Spliethoff and S. Fendt, *Energy Conversion and Management*, 2022, **274**, 116424.

106   S. Kreidelmeyer, H. Dambeck, A. Kirchner and M. Wünsch, *Kosten und Transformationspfade für strombasierte Energieträger,* available at: https://www.bmwk.de/Redaktion/DE/Downloads/Studien/transformationspfade-fuer-strombasierte-energietraeger.pdf?__blob=publicationFile, accessed 23 August 2023.

107   L. Wang, M. Chen, R. Küngas, T.-E. Lin, S. Diethelm, F. Maréchal and J. van Herle, *Renewable and Sustainable Energy Reviews*, 2019, **110**, 174–187.

108   G. Cinti, A. Baldinelli, A. Di Michele and U. Desideri, *Applied Energy*, 2016, **162**, 308–320.

109   M. Mozaffarian and R. W. R. Zwart, *Feasibility of biomass / waste-related SNG production technologies*, 2003.

110   E. Barbuzza, G. Buceti, A. Pozio, M. Santarelli and S. Tosti, *Fuel*, 2019, **242**, 520–531.

111   G. Song, S. Zhao, X. Wang, X. Cui, H. Wang and J. Xiao, *Case Studies in Thermal Engineering*, 2022.

112   K. R. Putta, U. Pandey, L. Gavrilovic, K. R. Rout, E. Rytter, E. A. Blekkan and M. Hillestad, *Front. Energy Res.*, 2022, **9**.

113   K. Melin, H. Nieminen, D. Klüh, A. Laari, T. Koiranen and M. Gaderer, *Front. Energy Res.*, 2022, **10**.

114   E. Anetjärvi, E. Vakkilainen and K. Melin, *0360-5442*, 2023, **276**, 127202.

115   F. Habermeyer, J. Weyand, S. Maier, E. Kurkela and R.-U. Dietrich, *Biomass Conv. Bioref.*, 2023.

116   B. Steinrücken, M. Dossow, M. Schmid, M. Hauck, S. Fendt, F. Kerscher and H. Spliethoff, in *36th International Conference on Efficiency, Cost, Optimization, Simulation and Environmental Impact of Energy Systems (ECOS 2023)*, ed. J. R. Smith, ECOS 2023, Las Palmas De Gran Canaria, Spain, 2023, pp. 1170–1181.

117   M. Pozzo, A. Lanzini and M. Santarelli, *Fuel*, 2015, **145**, 39–49.

118   F. Monaco, A. Lanzini and M. Santarelli, *Journal of Cleaner Production*, 2018, **170**, 160–173.

119   L. R. Clausen, G. Butera and S. H. Jensen, *0360-5442*, 2019, **172**, 1117–1131.

120   L. R. Clausen, G. Butera and S. H. Jensen, *0360-5442*, 2019, **188**, 116018.

121   G. Butera, S. H. Jensen, R. O. Gadsboll, J. Ahrenfeldt and L. R. Clausen, *Chemical Engineering Transactions*, 2019, **76**, 1177–1182.

122   G. Butera, S. Højgaard Jensen, R. Østergaard Gadsbøll, J. Ahrenfeldt and L. Røngaard Clausen, *Fuel*, 2020, **271**, 117654.

123   C. Malins, Searle, Stephanie, Baral, Anil, D. Turley and L. Hopwood, *Wasted - Europe's untapped resource,* available at: https://theicct.org/sites/default/files/publications/WASTED-final.pdf, accessed 23 August 2023.

124   The World Bank, *Land area (sq. km) - European Union,* available at: https://data.worldbank.org/indicator/AG.LND.TOTL.K2?end=2020&locations=EU&start=2008, accessed 29 August 2023.

125   BP, *bp Statistical Review of World Energy,* available at: https://www.bp.com/content/dam/bp/business-sites/en/global/corporate/pdfs/energy-economics/statistical-review/bp-stats-review-2022-full-report.pdf, accessed 23 August 2022.

126   Umweltbundesamt, *Kohlendioxid-Emissionsfaktoren für die deutsche Berichterstattung atmosphärischer Emissionen,* available at: https://www.umweltbundesamt.de/sites/default/files/medien/361/dokumente/co2_ef_liste_2022_brennstoffe_und_industrie_final.xlsx, accessed 25 August 2023.

127   C. Hamelinck and M. Bunse, *Carbon footprint of methanol,* available at: https://www.studiogearup.com/wp-content/uploads/2022/02/2022_sGU-for-MI_Methanol-carbon-footprint-DEF-1.pdf, accessed 25 August 2023.

128   G. S. Forman, T. E. Hahn and S. D. Jensen, *Environmental science & technology*, 2011, **45**, 9084–9092.

129   *Carbon Footprint-Country specific electricity grid greenhouse gas emission factors,* available at: https://www.carbonfootprint.com/docs/2023_02_emissions_factors_sources_for_2022_electricity_v10.pdf, accessed 25 August 2023.

130   Methanol Institute, *Methanol Price and Supply/Demand,* available at: https://www.methanol.org/methanol-price-supply-demand/, accessed 23 August 2023.